J. Membrane Biol. 134, 241–250 (1993)

The Journal of
Membrane
Biology

Independence of Water and Solute Pathways in Human RBCs

Robert I. Macey, Daniel M. Karan
Department of Molecular and Cell Biology, University of California, Berkeley, California, 94720

Received: 24 September 1992/Revised: 18 December 1992

Abstract. We have investigated the permeability of the human red blood cell to four di-hydroxy alcohols, 1,2PD (1,2 propanediol), 1,3PD (1.3 propanediol), 1,4BD (1,4 butanediol), and 2,3BD (2,3 butanediol), and to water by using a recently developed ESR stopped-flow method which is free from artifacts found in light scattering methods. Numerical solutions of the Kedem-Katchalsky equations fit to experimental data yielded the following permeability coefficients: $P_{1,2PD} = 3.17 \times 10^{-5}$ cm sec^{-1}, $P_{1,3PD} = 1.75 \times 10^{-5}$ cm sec^{-1}, $P_{1,4BD} = 2.05 \times 10^{-5}$ cm sec^{-1}, $P_{2,3BD} = 7.32 \times 10^{-5}$ cm sec^{-1}. Reflection coefficients (σ) were evaluated by comparing data fit with assumed values of $\sigma = 0.6, 0.8$ and 1.0. In all four cases the best fit was obtained with $\sigma = 1.0$. Treatment of cells with PCMBS (para-chloro mercuri-benzene-sulfonate) was followed by a large (>10-fold) decrease in water permeability with virtually no change in alcohol permeability. We conclude that these alcohols do not permeate the water channels to any significant extent, and discuss some of the problems in light scattering measurements of reflection coefficients that could lead to erroneous values for σ.

Key words: Red blood cells — Erythrocytes — Reflection Coefficient — Alcohol — Permeability — Water

Introduction

The resolution of transport pathways for small di-hydroxy alcohols through the human red cell membrane has not found universal agreement. Aside from its own intrinsic interest, the issue is important because it has implications about transport mechanisms for other solutes (Mayrand & Levitt, 1982; Levitt & Mlekoday, 1983; Toon & Solomon, 1987) and water (Macey & Farmer, 1970; Macey, Karan & Farmer, 1972; Macey, 1979; Solomon et al., 1983). Many years ago we published our observations that the permeability of several di-hydroxy alcohols did not change when water permeability was substantially inhibited by PCMBS (para-chloro mercuribenzene-sulfonate). We concluded that these alcohols do not permeate the water channels to any significant extent. This conclusion appears to have been overlooked; small di-hydroxy alcohols have been used repeatedly (Sha'afi, Gary-Bobo & Solomon, 1971; Solomon et al., 1983; Toon & Solomon, 1987, 1990) in an attempt to probe the properties of water channels.

Unfortunately, our PCMBS experiments based on light scattering measurements of volume perturbations induced by osmotic challenges were reported in a preliminary note and in a symposium (Macey & Farmer, 1970; Macey et al., 1972) without a full-length paper detailing experimental methods and results. To our knowledge these observations have never been refuted nor have they been repeated. More recently we have developed an accurate ESR method for measurements of volume perturbations that is free from many of the artifacts associated with stopped-flow light scattering. Rather than resurrecting data collected many years ago, we have taken this opportunity to restudy the problem using improved analytical as well as experimental techniques.

While it is reasonable to argue that an intact water transport in the presence of blocked solute transport does not prove independence of transport

Correspondence to: R.I. Macey

pathways, the converse is not true. Our position is that if the permeability of these alcohols does not show substantial reductions when the water channels are blocked, then the alcohol and water pathways are independent. If the pathways are independent, then the reflection coefficients of the alcohols should equal one (except for the small correction imposed by the distinction between water and volume flow). This suggests that methods used for those measurements of alcohol reflection coefficients that differ substantially from unity should be subjected to close scrutiny. It would follow that the results of this paper have consequences for sigma measurements extending to solutes beyond those considered in this paper.

Materials and Methods

Our experimental method for measuring transient red cell volume changes by stopped-flow ESR has been described in an earlier publication (Moronne et al., 1990). Briefly, it consists of monitoring the ESR signal of a rapidly penetrating spin label while extra cellular signals are obliterated by a quenching reagent. This permits changes in *intracellular* signal to be determined with ease. If the rate of spin label permeation is much faster than water, then, on the time scale of our experiments, the spin label will be in quasi-equilibrium at all times. If cell volume increases, the spin label will immediately enter the cell, increasing the number of internal spins and keeping the internal concentration invariant. It follows that cell volume is proportional to the total number of spin label within the cell which in turn is a linear function of the ESR signal. Control experiments show that alcohol by itself does not affect the ESR signal in the absence of cell membranes. Experiments performed using 1,3 propanediol over concentrations ranging from 0 to 200 mM showed no change in the ESR midpeak signal height.

We have modified the method by replacing our former spin label Tempone (2,2,6,6-tetramethylpiperidone-N-oxyl) with the more rapidly permeating label Tempo (2,2,6,6-tetramethylpiperidine-N-oxyl; permeation time constant of approximately 3.8 msec—*see* Results). In addition, we used 30 mM Potassium Manganese EDTA as the quenching reagent. This concentration was chosen to optimize spin probe quenching as well as to provide an osmotic balance for intracellular hemoglobin.

Possible effects of Potassium Manganese EDTA on water or alcohol permeability were tested. This control required an independent method that could be used both with and without the quencher. Stopped-flow light scattering was used to measure relaxation times in response to equal small osmotic perturbations produced in the presence and absence of quencher. P_f controls were obtained by cell volume swelling from 290 mOsm (impermeable solute) to 260 mOsm (impermeable solute). Time constants in the absence of quencher averaged 415 msec, corresponding to $P_f = 0.019$ cm/sec. In the presence of quencher, time constants were essentially the same averaging 407 msec. P_S controls were obtained by cell volume swelling from 290 mOsm (impermeable solute) to 260 mOsm (impermeable solute) + 30 mOsm 1,3 propanediol. Time constants which reflect the alcohol permeation were 2.37 sec in the absence of quencher and 2.13 sec with quencher present. The quencher has no significant effect on water or alcohol permeability.

Further, stopped-flow was implemented with a computer-controlled stop-flow using three independently driven syringes manufactured by Bio-Logic. This allowed us to divide each experiment into two consecutive phases in order to make independent measurements of osmotic water permeability (Phase 1) and solute permeability (Phase 2) within seconds of one another.

Blood Preparation

Freshly expired blood obtained from the local blood bank was washed several times in isotonic buffered KCl with a final wash in the "cell suspension solution" (*see* Table 1). Cells were then re-suspended in the cell suspension solution to a 20% hematocrit. For PCMBS experiments the red cells were re-suspended in the cell suspension solution containing 2 mM PCMBS and experiments were begun after 35 min incubation (full inhibition) at room temperature.

Experimental Procedure

Composition of solutions used in these experiments are listed in Table 1. Typically syringe 1 contained the P_f solution, syringe 2 contained the P_S solution, and syringe 3 contained the 20% hematocrit cell suspension. The two phases of the experiment were obtained by alternately mixing 750 μl from syringe 3 (cells) with an equal volume from syringe 1 (P_f solution) and after a preset time, mixing another 750 μl from syringe 3 (cells) with an equal volume from syringe 2 (P_S solution).

Following Fig. 1 in temporal order, the first phase consists of a mixing period lasting 0.6 sec during which 0.750 ml of hypotonic P_f solution ($\Pi = 0.48\ \Pi_{iso}$ where $\Pi_{iso} = 290$ mOsm) is mixed with 0.750 ml of 20% cells suspended in a hypertonic solution ($\Pi = 1.2\ \Pi_{iso}$) followed by the stopped-flow period, lasting 5.0 sec in untreated blood (30.0 sec in PCMBS-treated blood, see Fig. 5). Phase 1 gives the red cells' dynamic response to an osmotic "salt" gradient by swelling from the initial state at $\Pi = 1.2\ \Pi_{iso}$ to the final state at $\Pi = 0.8\ \Pi_{iso}$. Phase 1 is followed immediately by Phase 2. Again, a mixing period lasting 0.6 sec during which 0.750 ml from syringe 2 ($\Pi = 0.48\ \Pi_{iso}$ {salts} + $0.72\ \Pi_{iso}$ {alcohol}) is mixed with 0.750 ml from syringe 3 (20% hematocrit in $\Pi = 1.2\ \Pi_{iso}$ {salts}). This is followed by the second stopped-flow period, lasting from 13.8 to 48.8 sec depending on which alcohol is being tested and whether the cells are PCMBS treated or untreated. This stopped-flow period of Phase 2 gives the red cells' dynamic response to an osmotic "salt" plus alcohol gradient by swelling from the initial state at $\Pi = 1.2\ \Pi_{iso}$ to the final state at $\Pi = 0.8\ \Pi_{iso}$. Note from Table 1, Phase 2 that the osmolarity of the cell suspension is equal to the osmolarity of the final mix. As a result, initial changes in cell volume are undetectable and only begin to appear as solute enters the cell. The internal water content of the cells (or cell volume) is monitored during mixing and during stopped-flow for both phases by measuring the unquenched ESR signal intensity produced by the spin probe Tempo inside the red cells.

Data Analysis and Calibration

Water and solute fluxes induced by sudden osmotic perturbations of permeable solutes are described by the Kedem-Katchalsky equations. Applying these to corresponding volume changes in red cells leads to the following pair of differential equations.

Table 1. Measurement of P_f by swelling cells in hypotonic solution (Phase 1) and of P_s by swelling cells in the presence of alcohol (Phase 2)

Experimental condition	Cell susp 750 μl syringe 3	P_f soln 750 μl syringe 1	P_S soln 750 μl syringe 2	Final mixture
		Phase 1		
RBC HCT	20%			10%
KCl	141 mM	23.5 mM		76 mM
K_2MnEDTA	30 mM	30 mM		30 mM
K_2HPO_4/KH_2PO_4 pH = 7.4	10 mM	10 mM		10 mM
Tempo Alcohol		2 mM		1 mM
PCMBS	0 or 2 mM			0 or 1 mM
Osmolarity	348 mOsm	139 mOsm		232 mOsm
		Phase 2		
RBC HCT	20%			10%
KCl	141 mM		23.5 mM	76 mM
K_2MnEDTA	30 mM		30 mM	30 mM
$KHPO_4/KH_2PO_4$ pH = 7.4	10 mM		10 mM	10 mM
Tempo			2 mM	1 mM
Alcohol			209 mM	116 mM
PCMBS	0 or 2 mM			0 or 1 mM
Osmolarity	348 mOsm		139 mOsm "salt" + 209 mOsm alcohol	232 mOsm "salt" + 116 mOsm alcohol

$$\frac{dv}{dt} = P_f \overline{V_w} C_{iso}\left[\frac{A}{V_{iso}}\right]\left[\frac{1-b_m}{v-b_m} - c_m^o + \sigma(c_s - c_s^o)\right]$$

$$\frac{dc_s}{dt} = \frac{[(1-\sigma)\bar{c}_s - c_s]\frac{dv}{dt} + P_s[c_s^o - c_s]}{v - b_s}$$

where: v is the cell volume relative to isotonic conditions; P_f is the osmotic water permeability coefficient; $\overline{V_w}$ is the partial molar volume of water; C_{iso} is the isotonic osmolarity (290 mOsm); A is the surface area of the cell (1.37×10^{-6} cm^2); V_{iso} is the isotonic cell volume (84×10^{-12} cm^3); b_m is the "osmotic dead space" = 0.42 V_{iso}; c_m^o is the impermeant extracellular osmolarity relative to isotonic conditions; σ is the reflection coefficient; c_s is the intracellular permeant solute concentration normalized to isotonic; c_s^o is the extracellular permeant solute concentration normalized to isotonic; $\bar{c}_s$ is the normalized mean solute concentration across the cell membrane; P_S is the solute permeability coefficient; b_S is the intracellular volume fraction unavailable for solute distribution = 0.34 V_{iso}.

Parameter estimates were obtained by least squares fit of the numerical solutions of these equations to experimental data (adjusted to correct for the small deadtime lag of 28 msec). Equations were solved using an Euler integration routine, and least squares fit utilized a Parafit Algorithm (Ruckdeschel, 1981) Implementation requires a calibration converting ESR signals into normalized cell volume, v. Figure 2 shows that ESR signal is a linear function of v. This allows us to calibrate each trace individually by using initial and final volumes (calculated from impermeant solute osmolarities) with corresponding ESR signals.

The initial ESR signal at time zero (actually time = 28 msec) was obtained from the latter portions of the flow signal while initial v was calculated from the osmolarity of the cell incubation solution (prior to mixing in the stopped-flow). In Phase 2 traces (designed to measure P_S), the initial extracellular challenge consists of a solution that is isosmotic with respect to the internal cell contents; cell volume changes only as the relatively slowly permeating alcohol enters. As a result, volume changes during the first 28 msec are negligible and our use of ESR flow signal to approximate the initial value is very accurate. Similarly in those Phase 1 traces where water flow is inhibited by PCMBS, the volume change is imperceptible over the first 28 msec. In Phase 1 control traces where water movements are rapid (time constants of the order of 280 msec) volume changes within the first 28 msec are small but measurable. However, corrections for this time discrepancy by extrapolating back to true zero time had virtually no effect on our recovered values for P_f.

The final ESR signal, at time "infinity," was obtained from the asymptote of the raw data while the final v was calculated from the osmolarity of impermeable solutes in the final equilibrium solution (following mixing in the stopped-flow). Some traces showed a very small linear drift of unknown origin. As a result we examined two alternative corrections to all data. In one, measured control iso-volume "baselines" (obtained by mixing cells with isosmotic salt solutions in the stopped-flow) were subtracted from the data. In the other case the last 10 to 15% of each asymptote was fit with a linear least square line which was then subtracted from the data. Both methods gave similar results. We opted for the latter method simply because it was consistent

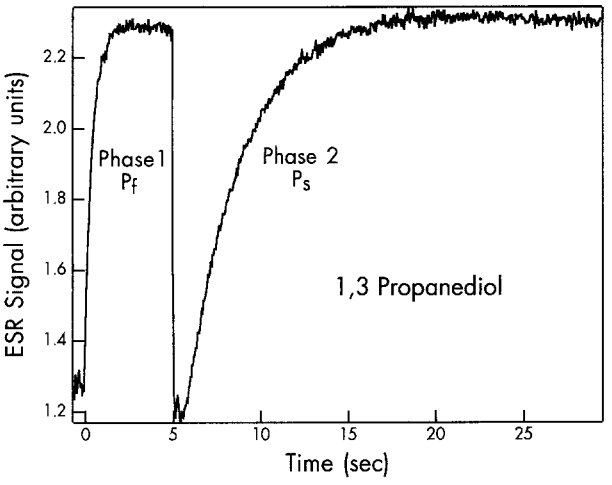

Fig. 1. A typical sequence of two stopped-flow measurements, Phase 1 and Phase 2. Flow and mixing takes place during the initial 0.6 sec of each phase, after which the flow is stopped. Phase 1 shows the osmotic response of cell volume (in ESR units) to a hypotonic "salt" challenge yielding Pf, the water permeability. 750 μl of 20% cells equilibrated with a hypertonic solution (Table 1, syringe 3) are mixed with 750 μl of hypotonic challenging solution (Table 1, syringe 1). Phase 2 shows the osmotic response when 750 μl of 20% cells equilibrated with the same hypertonic solution (Table 1, syringe 3) are mixed with 750 μl of isosmotic challenging solution containing "salt" and 1,3 propanediol (Table 1, syringe 2). The analysis of Phase 2 yields Ps and σ, the alcohol permeability and reflection coefficient, respectively.

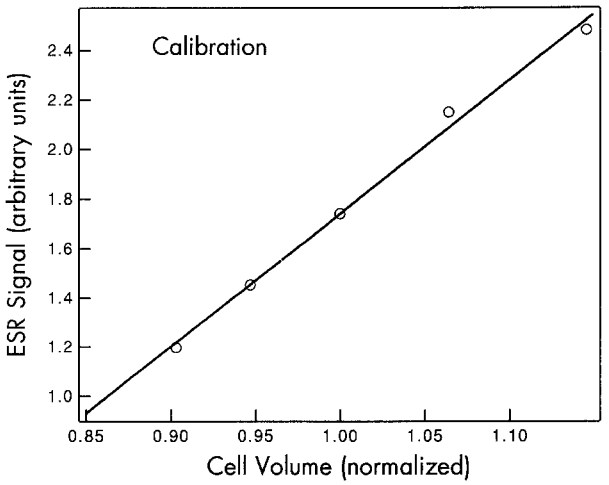

Fig. 2. The linearity of the ESR signal from the intracellular spin probe Tempo *vs.* the normalized cell volume over the range of volume changes used in our experiments. Cell volume was changed by equilibration in solutions of varying osmolarities. Normalized cell volume was calculated from solution osmolarities.

with our other efforts to avoid extrapolating results of one trace to "correct" the data of another.

To extract parameters from the data, we found it most efficient to search for one parameter at a time. In Phase 1 experiments this was straightforward because P_f is the only unknown parameter. In Phase 2 experiments both σ and P_S are unknown. Here we take advantage of the fact that $0 < \sigma < 1$, and that 10% errors in *measured* values of σ in red cells are insignificant. It then becomes a simple matter to fix the value of σ at each of a small series of numbers between 0 and 1, say 0.6, 0.8, and 1.0, and to examine the fit of each case individually along with its corresponding least squares estimate of P_S.

Results

Deadtime Determination

After the 20% blood suspension and the appropriate challenge solution is mixed, it travels a short distance in a quartz tube through the center of the ESR microwave cavity and then exits. By simple calculations involving the distance to the center of the cavity from the mixer and the cross sectional area of the tube (obtained from the measured inner diameter as well as by filling with mercury and weighing), the deadtime (time it takes the fluid to travel from the T-mixer to the center of the cavity where its properties are measured) is easily determined. For a total of 1.5 ml (0.750 ml from each syringe) with a flow time of 0.6 sec, the deadtime calculates by both measurements to be 28 msec. This of course assumes that the fluids mix perfectly so that we are 28 msec into the reaction by the time the fluid reaches the observation port (center of the cavity). If the fluids mixed imperfectly, the actual time into the reaction would be less than 28 msec at the time of observation.

Tempo Permeability

A continuous flow experiment was employed to determine the Tempo permeability. A 20% hematocrit isotonic blood suspension containing no Tempo was mixed with an isotonic solution containing 2 mM Tempo and quencher. Flow velocity was varied over a fivefold range yielding observation times of 7.0 to 35.0 msec following initial mixing (*see* Fig. 3). The time zero point (external quenched signal only) was obtained by replacing the blood suspension in the experiment with an isotonic solution containing quencher, but no cells and no Tempo. All data points in Fig. 3 were averages taken during the latter half of the continuous flow phase for the highest accuracy. The points on the graph at 7.0 and 9.33 msec are slightly lower than their true values due to hemolysis produced by such high flow rates (a flow time of 0.6 sec with deadtime = 28 msec used in all other

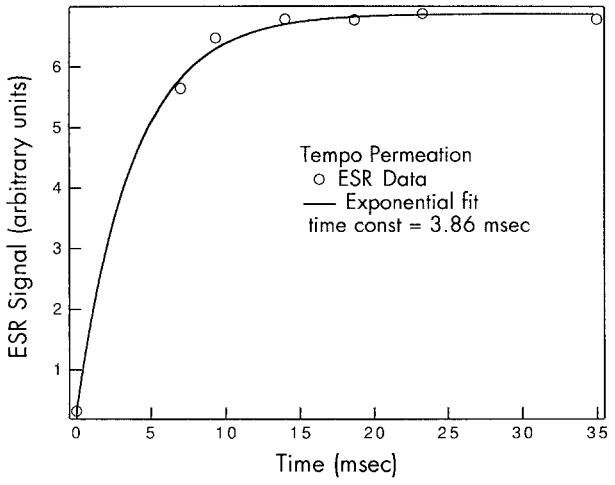

Fig. 3. Intracellular ESR signal from the rapid entry of Tempo *vs.* the amount of time the cells were exposed to the spin label. The time of exposure was varied by changing the rate of flow through the mixer, thus changing the time to the center of the microwave cavity (deadtime) where the signal was measured. The actual time constant for Tempo permeation is less than 3.86 sec, which was found to be an upper limit. *See text* for detail.

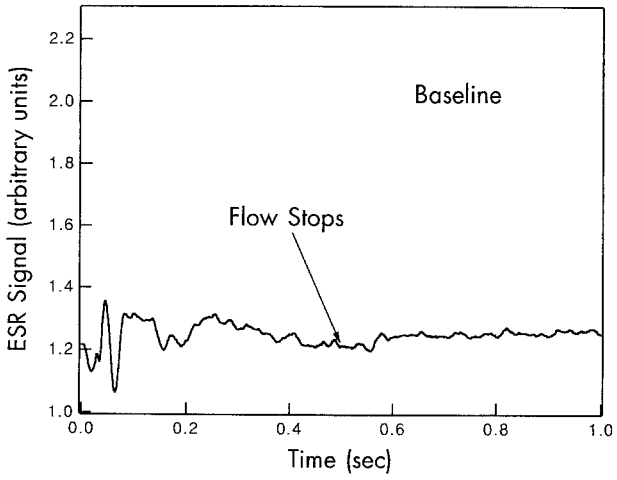

Fig. 4. Baseline graph showing 500 msec of continuous flow and 500 msec of stopped flow. From the constancy of the continuous and stopped-flow portions of these data it is easily seen that no visible artifacts are produced in the transition from flow to stopped flow.

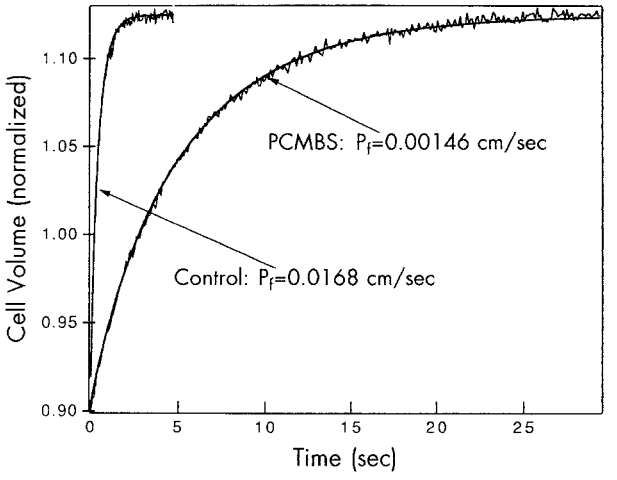

Fig. 5. The inhibition of water permeability by the mercurial PCMBS is illustrated by the two traces showing the treated and untreated red cells' response to mixing with the P_f solution (Table 1).

experiments provides a comfortable margin against hemolysis). An exponential fit through all the points yields a time constant of 3.86 msec which is greater than the actual value and is thus the upper limit. This rapid equilibration allowed us to place Tempo in the challenge solution only. This is desirable because the spin label is not degraded by long-term contact with hemoglobin prior to the experiment.

Mixing Artifact

An example of continuous plus stopped-flow data (average of 8 runs) seen in Fig. 4 illustrates the absence of significant mixing artifacts. The record shows 500 msec of continuous flow and 500 msec of stopped flow. From the constancy of the continuous and stopped-flow portions of these data it is easily seen that there are no visible artifacts produced in the transition from flow to stopped flow.

PCMBS Effect on Water and Alcohol Permeability

Typical data demonstrating inhibition of osmotic water flow by PCMBS are shown in Fig. 5 where the water permeability is decreased by more than a factor of 10 under the influence of PCMBS. The apparent effect of PCMBS on the solute 1,3 propanediol is shown in Fig. 6. The time course of volume change due to the alcohol permeation appears to be slowed down under the influence of PCMBS. However, results of data analysis (Table 2), show this slowing effect is related only to the fact that the water transport has been slowed down and not to any significant change in the solute permeability. The effect of PCMBS on water permeability and on the permeability of the four alcohols is shown graphically in Fig. 7. The values for the average permeabilities obtained for each alcohol from five different blood samples are given in Table 2 along with the standard deviations.

As seen graphically in Fig. 7 and from the data

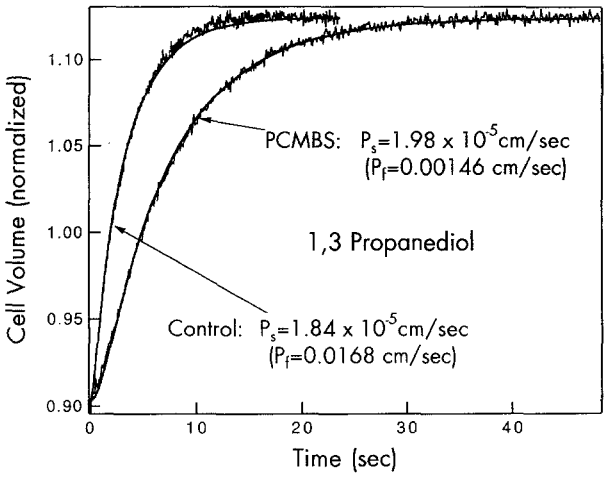

Fig. 6. PCMBS treated and untreated red cells' response to a combined "salt' and 1,3 propanediol challenge (P_S solution). The treated cells' response appears slower than untreated cells. This is due entirely to the inhibited water permeability, and not to a change in the alcohol permeability.

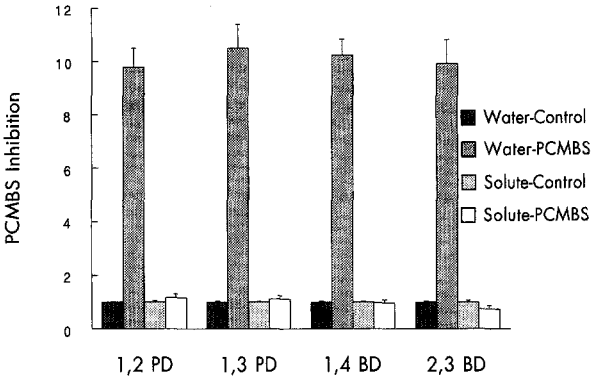

Fig. 7. Summary of all the permeability results for both PCMBS treated and untreated (control) cells for all four alcohols tested, 1,2 propanediol, 1,3 propanediol, 1,4 butanediol, and 2,3 butanediol. In this histogram both the solute and water controls are normalized to 1.0 and the inhibition due to PCMBS is shown relative to 1.0 with the appropriate error bars. PCMBS Inhibition $\equiv P_S$(control)/P_S(treated). PCMBS strongly inhibits water transport and has essentially no inhibitory effect on transport of alcohols.

Table 2. Data analysis of PCMBS effect on water and alcohol permeability

Alcohol	P_f(control) cm/sec	P_f(PCMBS) cm/sec	P_S(control) (10^{-5} cm/sec)	P_S(PCMBS) (10^{-5} cm/sec)
1,2 Propanediol	0.0156 ± 0.0005	0.0016 ± 0.0001	3.168 ± 0.222	2.912 ± 0.452
1,3 Propanediol	0.0160 ± 0.0006	0.0015 ± 0.0001	1.748 ± 0.054	1.560 ± 0.224
1,4 Butanediol	0.0170 ± 0.0007	0.0016 ± 0.0001	2.046 ± 0.078	2.118 ± 0.257
2,3 Butanediol	0.0160 ± 0.0006	0.0016 ± 0.0001	7.322 ± 0.514	10.23 ± 1.74

Each permeability represents data gathered with five different blood samples (6 to 10 repeats per sample). Errors are standard deviations of data.

summary in Table 2, the water pathway is essentially shut down, but the pathways for alcohol permeation are virtually unaffected by PCMBS treatment. This by itself is strong evidence that water and the four alcohols tested traverse the membrane by unrelated pathways. Within this context, the slight *increase* in 2,3 butanediol permeability under the influence of PCMBS does not appear to be significant.

The Reflection Coefficient

Additional evidence supporting independent pathways for water and alcohols in uninhibited cells comes from our values of σ for all four alcohols tested. For example, Fig. 8 shows data (average of many runs) for 1,2 propanediol fit with three different assumed values for σ. The LSQ fit to the data for each assumed σ is seen along with the solute permeability found for that σ. It is clear that $\sigma = 1.0$ provides the only acceptable fit to the data. Similar results (i.e., best fit with $\sigma = 1.0$) are shown in Figs. 9, 10, 11 for the other three alcohols. This is in disagreement with the findings of Toon and Solomon (1990) and is addressed in the Discussion.

Discussion

Independence of Water and Alcohol Pathways: Comparisons with Bilayers

Our permeability values for 1,2 propanediol, 1,4 butanediol, and 2,3 butanediol are lower than published by Toon and Solomon (1990) and by (Sha'afi, Gary-Bobo & Solomon, 1971). Reasons for the discrepancy are not clear. However, it could be related to the earlier values being based on a minimum volume method which requires numerical estimation of the second derivative of an empirical curve at a single point (the minimum volume). We can only speculate

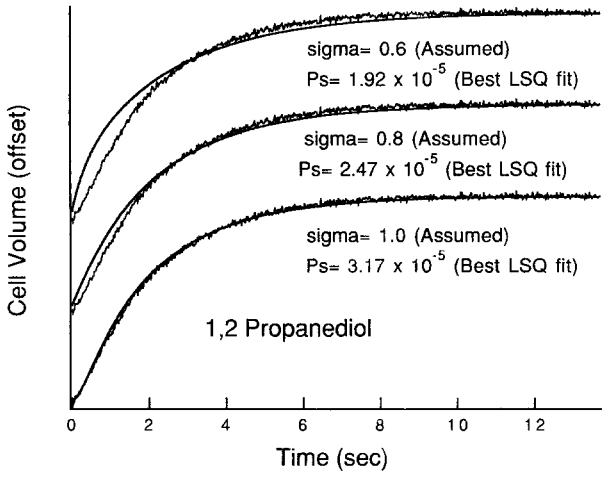

Fig. 8. Data from one experiment with 1,2 propanediol shown in triplicate and offset for ease of viewing. For each of these identical data traces a value of σ = 0.6, 0.8, or 1.0 was used along with the measured water permeability, to find the best least squares fit yielding P_S for the assumed value of σ. It is clear from the three graphs that only σ = 1.0 fits the data.

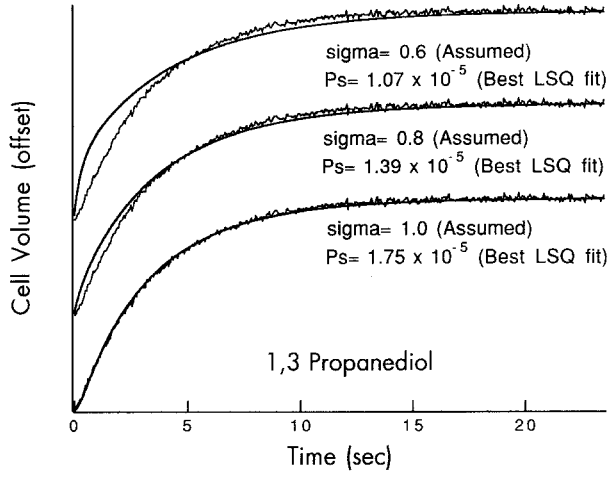

Fig. 9. Data from one experiment with 1,3 propanediol shown in triplicate and offset for ease of viewing. For each of these identical data traces a value of σ = 0.6, 0.8, or 1.0 was used along with the measured water permeability, to find the best least squares fit yielding Ps for the assumed value of σ. Again it is clear from three graphs that only σ = 1.0 fits the data.

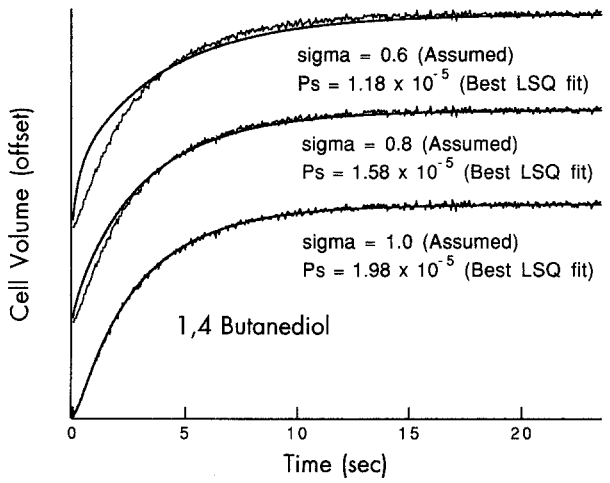

Fig. 10. Data from one experiment with 1,4 butanediol shown in triplicate and offset for ease of viewing. For each of these identical data traces a value of σ = 0.6, 0.8, or 1.0 was used along with the measured water permeability, to find the best least squares fit yielding Ps for the assumed value of σ. It is clear from the three graphs that only σ = 1.0 fits the data.

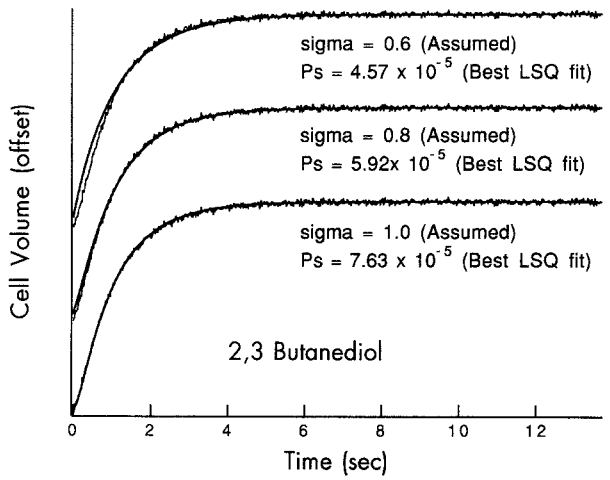

Fig. 11. Data from one experiment with 2,3 butanediol shown in triplicate and offset for ease of viewing. For each of these identical data traces a value of σ = 0.6, 0.8, or 1.0 was used along with the measured water permeability, to find the best least squares fit yielding Ps for the assumed value of σ. In this case, due to the faster permeability of 2,3 butanediol, it is more difficult to make the distinction between the fits for σ = 1.0 and 0.8 though on an expanded plot it shows that 0.8 does not fit as well as 1.0.

that the discrepancy in results is related to the difficulty in obtaining accurate values of the second time derivative of the cell volume at the time when the volume is at a minimum. We prefer our method which uses all data points, and without recourse to any numerical differentiation.

Our permeability values found for the four alcohols tested in red cells (1.75 to 7.32 $\times$ 10^{-5} cm/sec) are very close to measured or estimated permeability values for phosphatidylcholine-cholesterol bilayers (*see* Table 3). Finkelstein (1976) finds a value of 2.0 $\times$ 10^{-5} cm/sec for 1,4 butanediol in PC-cholesterol bilayers which compares favorably with the value 2.05 $\times$ 10^{-5} cm/sec we find in human red cells. For 1,2 propanediol we obtain an estimate of 2.07 $\times$ 10^{-5} cm/sec for a PC-cholesterol bilayer based

Table 3. Comparison of alcohol permeability (in units of 10^{-5} cm sec^{-1})

Alcohol	PC Bilayer[a]	PC + Cholesterol Bilayer[a]	RBC[b]	RBC[c]	RBC[d]
1,2 Propanediol	28	2.1[e]	7.11[f]		
	19.6[h]	1.47[h]	5.83[g]		3.17
1,3 Propanediol				2.94[f]	
				4.23[g]	1.75
1,4 Butanediol	27	2	5.40[f]	2.21[f]	
	18.9[h]	1.4[h]	4.43[g]	3.18[g]	2.05
2,3 Butanediol			17.42[f]	7.6[f]	
			14.28[g]	10.94[g]	7.32

[a] (Finkelstein, 1976.)
[b] (Toon & Solomon, 1990.)
[c] (Sha'afi, Gary-Bobo & Solomon, 1971.)
[d] This paper.
[e] Calculated from 1,4 butanediol ratio as (2/27) × 28.
[f] Original data.
[g] Data adjusted for consistency with cell area/volume assumed in this paper.
[h] Data adjusted for comparison with red cells by assuming 70% area available for diffusion (Branton & Deamer, 1972).

on measured values for a PC bilayer (Finkelstein, 1976), which again compares favorably with the red cell permeability of 3.17×10^{-5} cm/sec. Exact comparisons of permeabilities between red cells and bilayers cannot be taken literally because of variations in bilayer composition and symmetry. However, since the permeabilities of these alcohols in red cells are not appreciably different than the bilayer permeability, it is unnecessary to introduce any modification of the membrane by channels, carriers or other orifices to account for the transport of these solutes in red cells. In view of the variability of solute permeability with bilayer composition, even the higher permeabilities reported by Toon and Solomon (1990) require no special mechanism. In any case, it is clear that a substantial amount of alcohol permeation takes place through the bilayer. Use of gross permeability measurements to evaluate any proposed alternate pathway must take this into account explicitly. In our view alternate pathways make a minor contribution at best to transport of these alcohols.

Independence of Water and Alcohol Pathways: Reflection Coefficients

The reflection coefficient, σ, relates the coupling between water and solute flow through the membrane. A value of 1.0 indicates that water and solute flow are totally decoupled at the membrane, whereas a value of 0 indicates water and solute stay completely coupled and flow together through the membrane without any selectivity exerted by the membrane. An intermediate value indicates some degree of (de)coupling such as a membrane containing channels through which water and some, but not all, of the solute can pass. Using the ESR method described above, we have found that $\sigma = 1.0$ yields the best fit for all four alcohols tested. It is clear from the four graphs (Figs. 8, 9, 10, 11) that substantial deviations of data and best fit are apparent with $\sigma = 0.8$ and even worse with $\sigma = 0.6$. The simplest interpretation is that total decoupling takes place between the alcohols and water and that the alcohols do not travel through the water channels with the water.

Separation of Water and Alcohol Pathways: PCMBS Inhibition

The most compelling argument that the alcohols do not travel through the water channels is provided by the PCMBS data. It is seen from both Fig. 7 and Table 2 that the water transport is inhibited by a factor >10 and the solute permeability is not inhibited at all. Judging from the ratios of osmotic to diffusional water permeability, as well as from comparisons of activation energies and absolute permeability values, it is clear that PCMBS causes an all-or-none closure of water channels, and that when there is a 10-fold inhibition, virtually all of the water channels are closed (Macey et al., 1972; Moura et al., 1984). Yet, under these conditions alcohol permeability persists as though nothing happened. The conclusion that the major alcohol pathways are inde-

pendent of major water pathways in the red cell seems inescapable.

Measurements of Reflection Coefficients

If our conclusion that permeation pathways for water and alcohols are independent is correct, it remains to account for those observations that claim reflection coefficients are significantly less than one. The method devised and used by Toon and Solomon utilizes light scattering to monitor cell volume and depends on arriving at accurate estimates of the rate of cell volume change $(dV/dt)_{t=0}$ at the moment of mixing with an osmotically perturbing solution. If the perturbing solution is made exclusively of impermeable solutes then $(dV/dt)_{t=0} = P_f A(\Delta C_m)$. Plotting $(dV/dt)_{t=0}$ *vs.* ΔC_m gives a straight line with slope $= P_f A$. On the other hand, when the perturbing solution is made exclusively of permeable solutes then $(dV/dt)_{t=0} = P_f A\sigma(\Delta C_s)$, and a linear plot of $(dV/dt)_{t=0}$ *vs.* ΔC_S yields a slope of $P_f A\sigma$. Taking the ratio of these two slopes results in the desired value of σ. Because σ is obtained from a ratio, it would appear that many possible errors will cancel. Unfortunately not all.

Two strategies have been commonly used for error reduction: (i) signal averaging and (ii) baseline subtractions. While signal averaging will reduce random noise, it will do little to reduce systematic errors, and systematic erros (e.g., mechanical oscillations, mixing artifacts and index of refraction differences) require detailed consideration.

Light scattering techniques are always plagued with transient artifacts which affect at least the first hundred milliseconds of data after the flow is stopped. Baseline subtractions may correct some, but not all of these artifacts which depend on mechanical oscillations from rapid stopping (e.g., *see* Fig. 3 in Toon & Solomon, 1987, and Fig. 3 in Sha'afi et al., 1970) as well as tumbling of disc shaped cells and their subsequent relaxation (Blum & Foster, 1970; Mlekoday, Moore & Levitt, 1983). The artifacts are probably cell volume and shape dependent. There is no reason to expect them to be identical in suspensions where no volume change takes place (baselines) and in suspensions where cells undergo changes in volume and shape.

We have also encountered analytical difficulties when we attempted to repeat the $(dV/dt)_{t=0}$ method of Toon and Solomon (1990). Presumably, experimental conditions could be optimized by using the relatively artifact-free ESR method together with the slowly permeating di-hydroxy alcohols. However, our results were inconsistent; in our hands the time zero values of dV/dt are strongly dependent on which analytical function is used to fit the data as well as the number of data points used in the analysis. Often, the first few hundred milliseconds can be very well fit with a second-order polynomial, a third-order polynomial, or an exponential function. The value of the derivatives at time = 0 for each function, however, can be very different and usually is. Choosing any one method produced values of σ that were not repeatable and ranged above as well as below 1. Even with small systematic and/or random errors any procedure chosen to differentiate the data usually includes magnified information about the errors.

The ESR method and analysis we use does not have these problems: The optical index of refraction of the solutions does not play a role in our data acquisition or analysis. Further, the ESR method also has no problem with mixing or stopping artifacts (*see* Fig. 4). Finally, we fit the entire data curve without the need for finding the "right" analytic function or the "right" derivative at a single point in time. Although, in theory rate data (dV/dt) may be more sensitive to changes in certain parameters or conditions than integrated volume (V) data, in practice this sensitivity has already been lost or smoothed over in the observed V data. This sensitivity cannot be easily recovered by simple differentiation of empirical data.

We would like to thank Professor Lenore W. Yousef (Dept. of Biology, California State Univ., Fresno) for valuable discussions and critical comments. We thank Lidia Mannuzzu for measurements of ESR spectra in the presence and absence of alcohol. We are also indebted to Kate Van Fossen for her dedicated technical support. This work was supported by NIH grant No. HL-20985.

References

Blum, R.M., Foster, R.E. 1970. The water permeability of erythrocytes. *Biochim. Biophys. Acta.* **203:**410–423

Branton, D., Deamer, D. 1972. Membrane structure *In*: Protoplasmatologia II/E/I. M. Alfert, editor. pp. 1–70. Springer-Verlag, New York

Finkelstein, A. 1976. Water and nonelectrolyte permeability of lipid bilayer membranes. *J. Gen. Physiol.* **68:**127–135

Levitt, D.G., and Mlekoday, H.J. 1983. Reflection coefficient and permeability of urea and ethylene gycol in the human red cell membrane. *J. Gen. Physiol.* **81:**239–253

Macey, R.I., 1979. Transport of water and nonelectrolytes across red cell membranes. *In:* Transport across biological membranes, G. Giebisch, D.C. Tosteson and H.H. Ussing, editor, pp. 1–58. Springer-Verlag, Berlin-Heidelberg-New York

Macey, R.I., Farmer, R.E.L. 1970. Inhibition of water and solute permeability in human red blood cell. *Biochim. Biophys. Acta* **211:**104–106

Macey, R.I., Karan, D.M., Farmer, R.E.L., 1972. Properties of water channels in human red cells. *In:* Biomembranes.

Vol. 3. F. Kreuzer and J.F.G. Slegers, editors. pp. 331–334. Plenum, NY

Mayrand, R.R., Levitt, D.G. 1982. The urea and ethylene glycol facilitated transport systems in the human red cell membrane: saturation, competition, and asymmetry. *J. Gen. Physiol.* **81:**221–238

Mlekoday, H.J., Moore, R., Levitt, D.G. 1983. Osmotic water permeability of the human red cell. *J. Gen. Physiol.* **81:**213–220

Moronne, M., Miller, M., Mehlhorn, R., Macey, R.I. 1990. Static and dynamic measurements of intracellular water in red cells. *J. Membrane Biol.* **115:**31–40

Moura, T.F., Macey, R.I., Chien, D.Y., Karan, D.M., Santos, H. 1984. Thermodynamics of all-or-none water channel closure in red cells. *J. Membrane Biol.* **81:**105–111

Ruckdeschel, F.R. 1982. Basic Scientific Subroutines Vol II; pp. 75–82. McGraw-Hill, New York

Sha'afi, R.I., Gary-Bobo, C.M., Solomon, A.K. 1971. Permeability of red cell membranes to small hydrophilic and lipophilic solutes. *J. Gen. Physiol.* **58:**238–258

Sha'afi, R.I., Rich, G.T., Mikulecky, D.C., Solomon, A.K. 1970. Determination of urea permeability in red cells by minimum method. *J. Gen. Physiol.* **55:**427–450

Solomon, A.K., Chasan B., Dix, J.A., Lukacovic, M.F., Toon, M.R., Verkman, A.S. 1983. The aqueous pore in the red cell membrane: band 3 as a channel for anions, cations, nonelectrolytes and water. *Ann. N.Y. Acad. Sci.* **414:**97–123

Toon, M.R., Solomon, A.K. 1987. Interrelation of ethylene glycol, urea and water transport in the red cell. *Biochim. Biophys. Acta* **898:**275–282

Toon, M.R., Solomon, A.K. 1990. Transport parameters in the human red cell membrane: solute-membrane interactions of hydrophilic alcohols and their effect on permeation. *Biochim. Biophys. Acta* **1022:**57–71